**Nathan W. Luedtke**
**Yitzhak Tor**
*Department of Chemistry and Biochemistry, University of California, San Diego, La Jolla, CA 92093-0358*

*Received 4 March 2003; accepted 4 March 2003*

# Fluorescence-Based Methods for Evaluating the RNA Affinity and Specificity of HIV-1 Rev–RRE Inhibitors

***Abstract:*** *RNA plays a pivotal role in the replication of all organisms, including viral and bacterial pathogens. The development of small molecules that selectively interfere with undesired RNA activity is a promising new direction for drug design. Currently, there are no anti-HIV treatments that target nucleic acids. This article presents the HIV-1 Rev response element (RRE) as an important focus for the development of antiviral agents that target RNA. The Rev binding site on the RRE is highly conserved, even between different groups of HIV-1 isolates. Compounds that inhibit HIV replication by binding to the RRE and displacing Rev are therefore expected to retain activity across groups of genetically diverse HIV infections. Systematic evaluations of both the RRE affinity and specificity of numerous small molecule inhibitors are essential for deciphering the parameters that govern effective RRE recognition. This article discusses fluorescence-based techniques that are useful for probing a small molecule's RRE affinity and its ability to inhibit Rev–RRE binding. Rev displacement experiments can be conducted by observing the fluorescence anisotropy of a fluorescein-labeled Rev peptide, or by quantifying its displacement from a solid-phase immobilized RRE. Experiments conducted in the presence of competing nucleic acids are useful for evaluating the RRE specificity of Rev-RRE inhibitors. The discovery and characterization of new RRE ligands are described. Eilatin is a polycyclic aromatic heterocycle that has at least one binding site on the RRE (apparent* $K_d \approx 0.13$ $\mu$M*), but it does not displace Rev upon binding the RRE (*$IC_{50} > 3$ $\mu$M*). In contrast, ethidium bromide and two eilatin-containing metal complexes show better consistency between their RRE affinity and their ability to displace a fluorescent Rev peptide from the RRE. These results highlight the importance of conducting orthogonal binding assays that establish both the RNA affinity of a small molecule and its ability to inhibit the function of the RNA target. Some Rev–RRE inhibitors, including ethidium bromide,* $\Lambda$-$[Ru(bpy)_2eilatin]^{2+}$*, and* $\Delta$-$[Ru(bpy)_2eilatin]^{2+}$ *also inhibit HIV-1 gene expression in cell cultures (*$IC_{50} = 0.2$–$3$ $\mu$M*). These (and similar) results should facilitate the future discovery and implementation of anti-HIV drugs that are targeted to viral RNA sites. In addition, a deeper general understanding of RNA–small molecule recognition will assist in the effective targeting of other therapeutically important RNA sites.* © 2003 Wiley Periodicals, Inc. Biopolymers 70: 103–119, 2003

***Keywords:*** *RNA; pathogens; HIV-1; Rev response element*

## INTRODUCTION

RNA molecules exhibit vast structural and functional diversity, and are intimately involved in a wide range of biological activities, including information storage and chemical catalysis.[1] Site-specific recognition and binding of various RNAs by other cellular components often precede the catalytic events that are es-

*Correspondence to:* Yitzhak Tor; email: ytor@ucsd.edu
Contract grant sponsor: Universitywide AIDS Research Program (UARP) and National Institutes of Health (NIH)
Contract grant number: ID01-SD-027 (UARP) and AI 47673 (NIH)
Biopolymers, Vol. 70, 103–119 (2003)

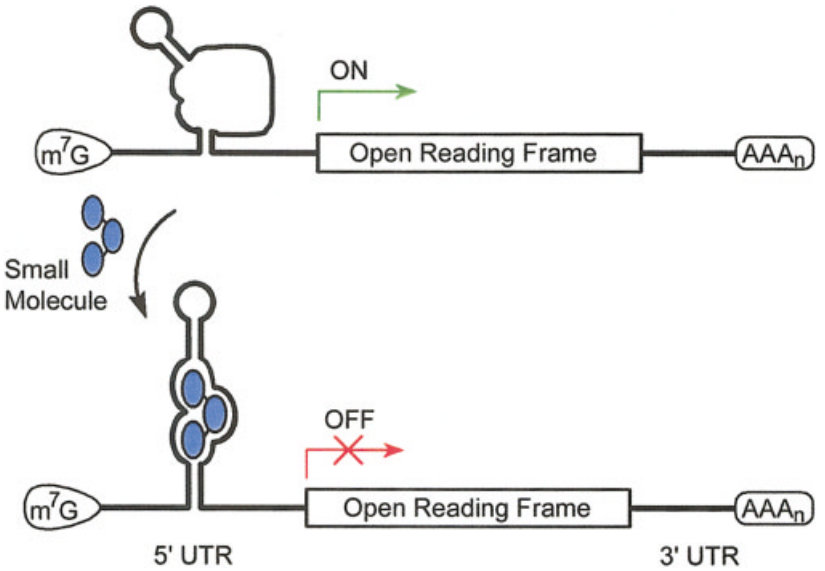


**FIGURE 1** A mature mRNA is actively translated in the absence of small-molecule binding (top). Upon binding of the 5′-UTR by its cognate small molecule, the translation of the gene is deactivated (bottom).[8–10] The mechanism proposed for this small molecule-dependent inactivation of mRNA translation involves a structural rearrangement of the 5′-UTR into a rigid complex that cannot be scanned by the ribosomal preinitiation machinery.[8–10]

sential to a wide range of activities, including initiation of DNA replication,[2] protein translation,[3] extension of telomereres,[4] splicing of heterogeneous nuclear RNAs,[5] and controlling the translational efficiencies of individual mRNAs.[6–10] In addition, RNA serves as the primary genome of many pathogenic viruses, including HIV.[11] Given the variety of potential targets, it is somewhat surprising that all the currently prescribed anti-HIV drugs are small organic compounds that bind to viral *proteins*.[12] RNA is beginning to emerge as an important, but currently underutilized, target for drug design.[13–16]

The translational efficiency of individual mRNA molecules is thought to be regulated at many levels, including the binding of the 5′- and 3′-untranslated regions (UTRs) of mRNA by proteins,[6] microRNAs,[7] and by small molecules.[8–10] Low molecular weight ligands that bind to and interfere with the function of individual mRNA molecules have been shown to control the translational efficiency, and hence the biological activities of downstream protein(s).[8–10] A conceptual proof demonstrating the ability of small organic molecules to regulate gene expression was first revealed in the context of an artificial gene construct.[8] An RNA aptamer located in the 5′-UTR of a mRNA was shown to inactivate the translation of a downstream reporter gene upon binding of its cognate small molecule (Figure 1).[8] Recent studies have shown that a number of natural metabolic systems are also regulated via small molecule–mRNA binding, resulting in the inactivation of mRNA translation in bacteria.[9,10]

## LIGAND SPECIFICITY

High binding specificity is a prerequisite for the effective in vivo modulation of RNA activity by a small molecule. Since nontargeted binding sites are typically found at much higher cellular concentrations than the desired RNA target(s), the cellular concentration of the free small molecule will dramatically suffer even if it has a moderate affinity to other cellular sites. Unintended binding interactions with tRNA, rRNA, DNA, proteins, phospholipids, or other cellular components, may also cause undesired effects including toxicity and mutagenicity. For the purposes of this discussion, the specificity of an RNA–ligand interaction will be defined by the binding affinity ($K_{eq}$) between a small molecule and a single RNA site, divided by its average affinity to "all" other potential binding sites [Eq. (1)]:

$$\text{Specificity} = \frac{K_{eq}\ (\text{interaction of interest})}{\text{Average } K_{eq}\ (\text{all other sites of interaction})} \quad (1)$$

For practical reasons, we use "specificity" as a relative term, where the affinity between a small molecule and its RNA "target" is weighted by its affinity to a number of arbitrary nucleic acids. The reported specificity is, therefore, always dependent on the selection of the "other" species used for the comparison. We have found that by quantifying a binding interaction

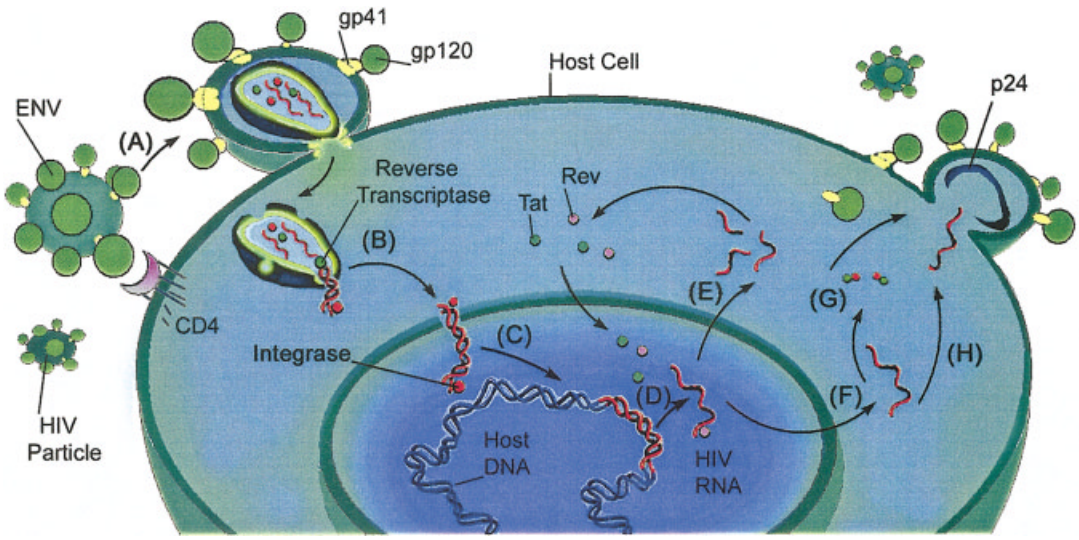


**FIGURE 2** The HIV-1 life cycle begins with the CD4-dependent invasion of the host cell (A). The viral particle "tricks" a CD4+ host cell with the gp120 domain of the "ENV" protein, which mimics a normal component of the human immune system (the major histocompatibility complex). Binding of CD4 to gp120 initiates endocytosis and results in the fusion of the viral and host membranes (A). Fusion is mediated by gp41 (the membrane-bound component of ENV). Upon fusion, the viral capsid is partially degraded and reverse transcriptase transcribes the 9 kilobase single-stranded viral RNA genome into double-stranded DNA (B). The double-stranded DNA copy of the HIV genetic code is then imported into the host's nucleus, where it is permanently integrated into the host's genome by integrase (C). At this point, viral activity can remain dormant for years. Eventually, an RNA copy of the HIV genome will be transcribed (D). Early in the replication cycle, this viral RNA becomes highly spliced, and it is translated into HIV regulatory proteins, including Rev and Tat (E). The Tat protein binds to its cognate RNA site (termed TAR) and facilitates the transcription of full-length HIV RNA (D); since Tat itself is an eventual product of this transcription, Tat's biosynthesis is in a positive feedback loop, leading to a rapid accumulation of viral RNA as well as the Tat and Rev proteins. Once the concentration of Rev is sufficient, it binds the HIV RNA at a site termed the Rev response element (RRE), and initiates HIV's "late replication" phase. The Rev protein polymerizes along RRE and facilitates the export of viral RNA out of the host nucleus while protecting the RNA from being spliced (F). From the unspliced and singly spliced HIV RNA, the proteins needed for viroid construction are translated (G). Unspliced RNA is then packaged into outgoing viral particles to serve as the primary genome (H).

in both the presence and absence of other nucleic acids, trends in the nucleic acid specificity of the RNA ligand become apparent.

## THE HIV LIFE CYCLE

HIV, the virus responsible for AIDS, relies upon the transcriptional and translational machinery of its host cell (Figure 2).[11] There are, however, a small number of protein–RNA interactions that are unique and essential to the HIV life cycle, including the Tat–TAR and Rev–RRE interactions.[17,18] Inhibition of these binding events should prevent the expression of viral proteins, and therefore stop replication of the virus. During the "early" replication phase of HIV, the viral RNA becomes highly spliced, from which a number of regulatory proteins, including Tat and Rev, are translated (step E, Figure 2). The Tat protein binds to a HIV RNA site termed TAR and facilitates the transcription of full-length viral RNA (step D, Figure 2). HIV's late replication phase is initiated by the Rev protein and its binding interactions with a HIV RNA site termed the RRE (Rev response element). By binding to the RRE, the Rev protein facilitates the export of HIV RNA out of the host nucleus, while protecting it from the cell's splicing machinery (step F, Figure 2).[19] The importance of this unspliced and singly spliced HIV RNA is 2-fold. First, it serves as an open reading frame for the "late-phase" proteins that are essential to the construction of new viral particles (step G, Figure 2). In addition, two copies of the unspliced HIV RNA are packaged into outgoing viroids, serving as their primary genome (step H,

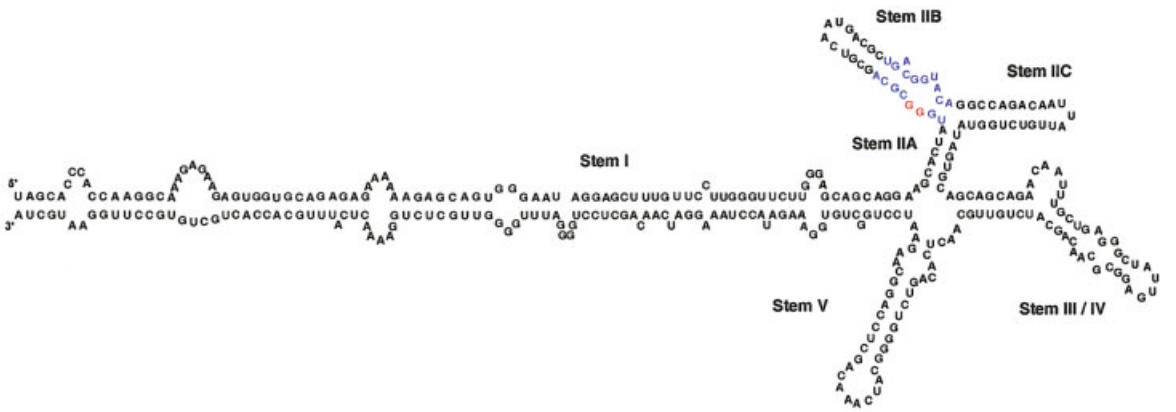


**FIGURE 3** The RRE, as defined by Mann et al.,[21] spans a total of 351 bases and contains a single high-affinity Rev binding site in Stem IIB (blue bases).[19] Deletion of two guanosine bases (red) prevents high affinity Rev binding to the entire RRE.[20,21]

Figure 2). Successful inhibition of Rev–RRE binding, therefore, should prevent the production of new viral particles by two separate mechanisms; the proteins essential for viroid construction are never translated, and the future HIV genomic RNA becomes highly spliced. Noncovalent (or competitive) inhibition of the Rev–RRE binding, however, might result in a higher cellular expression of both the Tat and Rev proteins, as Tat expression is in a positive feedback loop (steps D and E, Figure 2). Higher cellular concentrations of Rev may make the continued inhibition of Rev–RRE binding increasingly difficult, but a high cellular expression of Tat has been shown to induce apoptosis in a number of cell lines, including mammalian T-cells.[20] Competitive inhibition of the Rev–RRE interaction may, therefore, kill HIV-infected cells before the virus can replicate.

## THE REV–RRE INTERACTION

The RRE is a HIV RNA structure essential to viral replication.[19] The Rev protein binds to a single high-affinity site on stem II B of the RRE (red and blue bases, Figure 3). Following its binding to this site, additional Rev molecules bind cooperatively along stem I of the RRE in a stepwise fashion by utilizing both protein–protein and protein–RNA interactions.[21] Minimal mutations of the RRE within the primary Rev binding site have been reported to reduce the binding of the Rev protein to nonspecific levels (e.g., deletion of the red bases in Figure 3).[21,22] Without high-affinity Rev–RRE binding, the "late-phase" HIV proteins are not expressed, and the construction of new viral particles is halted (Figure 2).[23]

The RRE serves both as the high-affinity Rev binding site *and* as part of the open reading frame for the gp41 "fusion domain" of the ENV protein (Figure 2).[24] This dual role in the HIV life cycle is likely responsible for the unusually low mutation rate found at the primary Rev binding site on the RRE (Figures 4 and 5). Sequence alignment of 6 HIV-1 isolates from group M and two isolates from group O is shown in Figure 4.[25] A summary of our homology analysis for these isolates is shown in Figure 5. The variable RNA bases are indicated by stars, and the bases that are conserved have no symbol (Figure 5). Importantly, the bases that compose the primary Rev binding site are almost invariant between these genetically diverse groups of HIV isolates (blue bases Figure 5).

```
HXB2      GCACUAUGGGCGCAGCC.UCAAUGACGCUGACGGUACAGGCCAGACAAUUAUUGUCUGGUAUAGUGC
HXB3      GCACUAUGGGCGCAGCG UCAAUGACGCUGACGGUACAGGCCAGACAAUUAUUGUCUGGUAUAGUGC
SF2       GCACUAUGGGCGCAGUG.UCAUUGACGCUGACGGUACAGGCCAGACAAUUAUUGUCUGGUAUAGUGC
MAL       GCACGAUGGGCGCAGCG.UCACUAACGCUGACGGUACAGGCCAGACAGUUACUGUCUGGUAUAGUGC
ELI       GCACGAUGGGCGCA.CGGUCAGUGACGCUGACGGUACAGGCCAGACAAUUAAUGUCUGGUAUAGUGC
HIVU455   GCACAAUGGGCGCGGCG.UCAAUAACGCUGACGGUACAGGCCAGACAAUUAUUGUCUGGUAUAGUGC
HIVANT70  GCACUAUGGGCGCAGCG.GCAACAACGCUGGCGGUACAGACCCACACUUUGCUGAAGGGUAUAGUGC
MVP5180   GCACUAUGGGCGCAGCG.GCAACAGCGCUGACGGUACGGACCCACAGUGUACUGAAGGGUAUAGUGC
```

**FIGURE 4** RRE Stem II sequence alignments for 6 representative isolates from HIV-1 group M (HXB3, SF2, HXB2, MAL, ELI, HIVU455), and two isolates from HIV-1 group O (HIVANT70, MVP5180). Sequences and alignments were adopted from J-H Chen et al.[25] The bases that compose the high-affinity Rev binding site are shown in blue.[19]

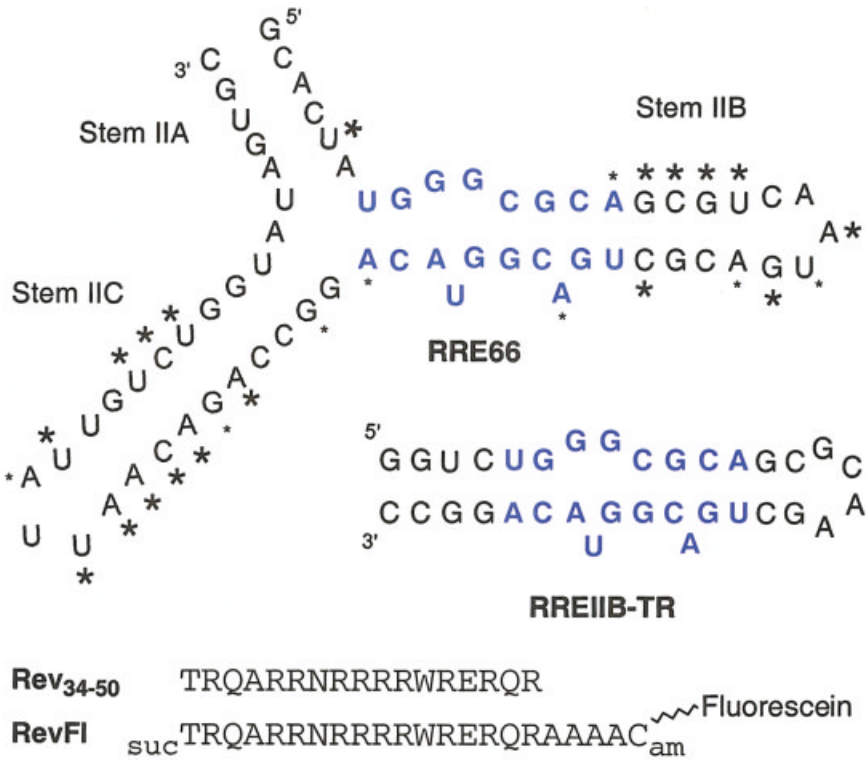


**FIGURE 5** Secondary structure of the 66 nucleotide RRE Stem II fragment "RRE66" from the HIV strain HXB3 that has been used in these studies. The bases essential for binding the first equivalent of Rev are shown in blue.[19] A summary of homology alignment for the HIV-1 groups from Figure 4 are shown: a large asterisk indicates a highly mutable position or alternate secondary structure, a small asterisk indicates conserved mutations only, and no asterisk indicates no variation. The peptide RevFl, used for fluorescence-based assays, is succinylated at its N-terminus, amidated at its C-terminus, and contains a four alanine spacer to fluorescein. These modifications have been shown to increase the helicity of this peptide, resulting in greater RRE affinity and specificity.[57] Indeed, the $Rev_{34-50}$ binding domain has been shown to bind the RREIIB-TR as an $\alpha$-helix both as a peptide,[50] and in the context of the full Rev protein.[58]

Interestingly, significant sequence and structural homologies are also found between the RREs of HIV-1 and HIV-2.[25] The primary Rev binding site on the RRE is, therefore, a highly attractive target for small molecule therapeutics, since small molecules that bind to and inactivate this site should possess consistent activities among diverse groups of HIV. In addition, the spontaneous mutations that can lead to drug resistance should be impeded by the dual function of the RRE.[26] For these reasons, we have sought small molecule Rev–RRE inhibitors that exhibit high affinity and high specificity for the primary Rev binding site on the RRE.

To evaluate the affinity and specificity of small molecules that are targeted to this site, we have used two different peptide displacement assays that utilize "RevFl," a fluorescent $Rev_{34-50}$ protein fragment (Figure 5). By monitoring the fluorescent signal of this peptide, its association to the RRE and subsequent displacement can be observed. The inhibition of Rev–RRE binding can thus be established in vitro.

## FLUORESCENCE POLARIZATION ANISOTROPY

Fluorescence anisotropy provides a useful tool to follow Rev–RRE association and inhibition.[27] The extent of fluorescence polarization (the "anisotropy" value) of the RevFl peptide is inversely proportional to its tumbling rate in solution. This tumbling rate is proportional to the total size and shape of RevFl, as well as to the temperature and viscosity of the solvent.[28] In theory, the fluorescence anisotropy of RevFl is an intrinsic property, and therefore not dependent on the total fluorescence intensity of the sample.[28] In practice, however, significant perturbations can be found at low emission intensities (Figure 6).[29] This effect is due, in part, to instrumental limitations, but is minimized by keeping the emission intensity of the sample above a certain threshold (100 arbitrary units for Figure 6).

As the RRE is titrated into a solution of RevFl, their association is observed by an increased anisot-

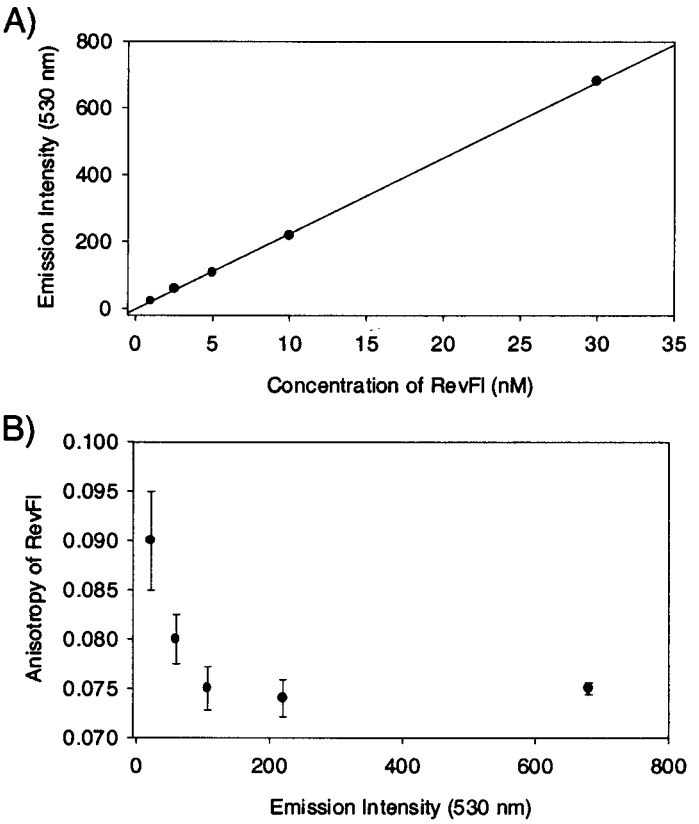


**FIGURE 6** Linear relationship between the concentration of the fluorescent peptide "RevF1" and the total fluorescence intensity (A). The apparent fluorescent anisotropy of the same five samples as a function of the total emission intensity of the sample (B). Error bars for anisotropy reflect the standard deviation of 10 anisotropy measurements made on the same day using the same sample of RevF1. The error bars only reflect, therefore, the errors related to the sampling by the instrument (Perkin Elmer LS-50B Luminescence Spectrometer). The largest sources of errors for the types of experiments described within this article are systematic errors associated with the quantification of both the macromolecules and small molecules used for the titrations (typically ±30%). Errors associated with volume and weight measurements are usually smaller and more random (typically ±20%). Errors associated with the instrument itself are much smaller and less random (typically ±5%), and can be minimized by taking the fractional change in anisotropy or emission intensity instead of absolute values.

ropy value (red data, Figure 7). Analysis of these data indicates that RevFl has a high affinity for the RRE66 ($K_d$ = ~3 n*M* at 22°C).[30] This is similar to the binding affinity between the full-length Rev protein and the RRE ($K_d$ = ~1 n*M*).[31,32] Using fluorescence anisotropy, the affinity of RevFl to a number of non-viral nucleic acids has also been measured. Both $tRNA^{Phe}$ and a mixture of yeast tRNAs ($tRNA^{mix}$) have approximately a 1000-fold lower affinity for RevFl ($K_d$ = ~2.4 $\mu M$) as compared to the RRE. Calf thymus (CT) DNA has approximately a 10,000-fold lower affinity to RevFl as compared to the RRE ($K_d$ = ~26 $\mu M$). Rev's high affinity for the RRE, combined with its low affinity to most other nucleic acids, confirms Rev's high specificity for the RRE [Eq. (1)].[31]

Once the Rev–RRE complex is partially formed (top, Figure 7), an inhibitor can be titrated (blue, Figure 7). Competitive inhibitors will bind to the RRE and shift the three-way binding equilibrium towards release of the free RevFl peptide (bottom left, Figure 7). If both the number of inhibitor binding sites in the Rev binding site *and* the stoichiometry for RevFl displacement are determined (or in some cases assumed), the absolute affinity of the RRE–"I" binding interaction can be calculated ($K_i$ is equivalent to $K_d$).[30,33,34] The curve fitting of raw displacement data to $K_i$ values has been used by some groups to minimize the errors associated with sampling noise and with nonsaturated binding isotherms.[33,34] In our experience, however, the uncertainties associated with binding stoichiometries, together with the errors as-

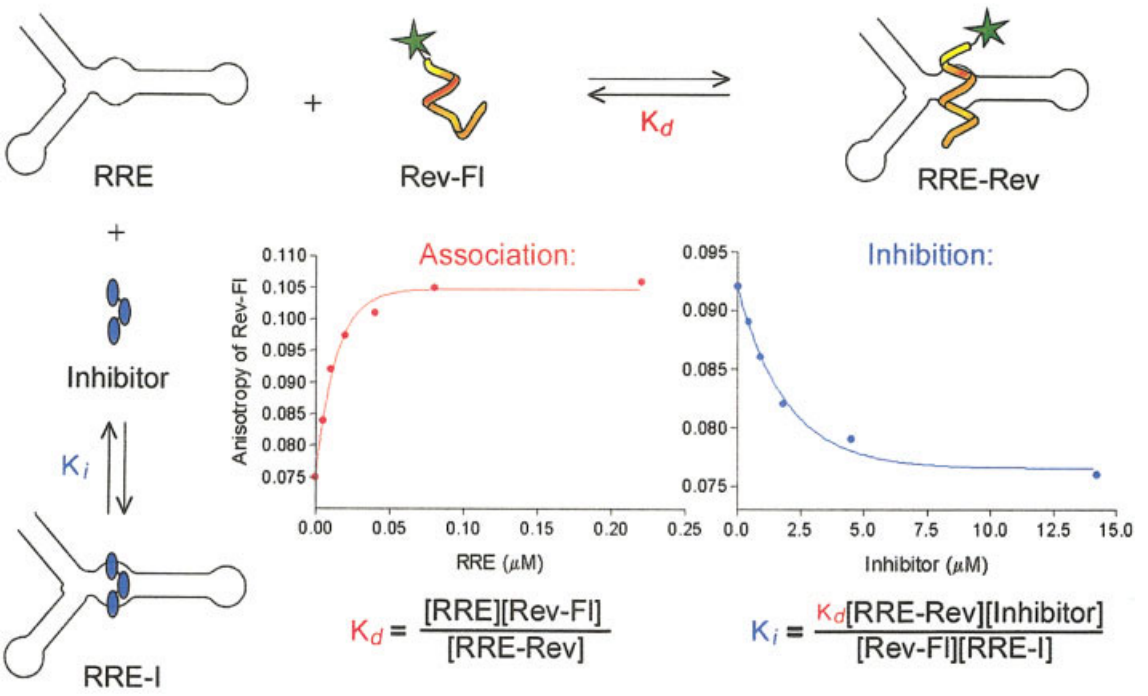


**FIGURE 7** Fluorescence anisotropy is used to monitor RevF1–RRE association (top) and inhibition (left). The fluorescence anisotropy of 10 n*M* of RevFl is monitored as RRE is titrated (red). Upon partial complex formation (10 n*M* of RRE), an inhibitor is added that displaces RevF1 from the RRE (blue). All binding experiments (including those using the solid-phase assay and emission spectroscopy) were conducted at 22°C in a buffer containing 30 m*M* HEPES (pH 7.5), KCl (100 m*M*), sodium phosphate (10 m*M*), $NH_4OAc$ (10 or 20 m*M*), guanidinium HCl (10 or 20 m*M*), $MgCl_2$ (2 m*M*), NaCl (20 m*M*), EDTA (0.5 m*M*), and Nonidet P-40 (0.001%). This complex mixture of cations and anions is found to minimize aggregation and the loss of cationic ligands onto surfaces, and it maximizes the reversibility of the Rev–RRE interaction (as evident in both anisotropy and solid-phase assays).

sociated with macromolecular and small molecule quantification, outweigh any gains in accuracy provided by curve fitting (at least for $K_i$ calculations; this is not necessarily true for simple two-component $K_d$ curve fitting). In almost all cases, however, the accuracy of the reported affinity dramatically improves when the concentration of the RNA target used in the experiment is approximately equal to or lower than its affinity ($K_d$) to the molecule that is being titrated, and when the binding stoichiometry is independently established using an orthogonal method.

A thorough investigation of both the binding stoichiometry and displacement stoichiometry of a ligand is often not possible. Its affinity to the Rev binding site on the RRE is, therefore, evaluated by measuring the concentration of inhibitor needed to displace ½ of Rev from the RRE (defined as its $IC_{50}$ value). $IC_{50}$ values are activity values that are proportional to $K_i$ values *if* the RRE binding and Rev displacement stoichiometries are similar for all ligands being evaluated. $IC_{50}$ values can easily be converted into $K_i$ values if the binding stoichiometry is known. For example, at 10 n*M* of RevFl and 100 n*M* of RRE, neomycin B (Figure 8) has an $IC_{50}$ value of 7 $\mu M$ (Table I). This value can be converted into a $K_i$ value of 0.20 $\mu M$ if one assumes a 1:1 stoichiometry for both binding and displacement (Figure 7). Under these conditions, $K_i$ (n*M*) $\approx$ ($IC_{50}$ − 94 n*M*)/34 n*M*.[35] A similar $K_i$ value for neomycin (0.15 $\mu M$) has been reported by Rando for the displacement of a rhodamine-labeled paromomycin molecule from a truncated RRE construct.[33] Tok also reports a $K_i$ of 0.18 $\mu M$ for neomycin binding to the RRE.[34] In addition, we have recently used a trace concentration (10 n*M*) of a BODIPY–neomycin conjugate and titrated the RRE66 to probe for neomycin's highest-affinity binding site on the RRE66, and have measured an apparent $K_d$ = 0.20 $\mu M$.[37] This assumes a 1:1 binding stoichiometry and is usually a reasonable assumption when the concentration of the fluorescent probe is low compared to its affinity to the species being titrated.[35] These results suggest that for the RRE66, neomycin's highest affinity (primary) binding site is disruptive to the binding of Rev (since the apparent $K_d = K_i$) . Experiments conducted by Marino, however, suggest, that neomycin's primary binding site

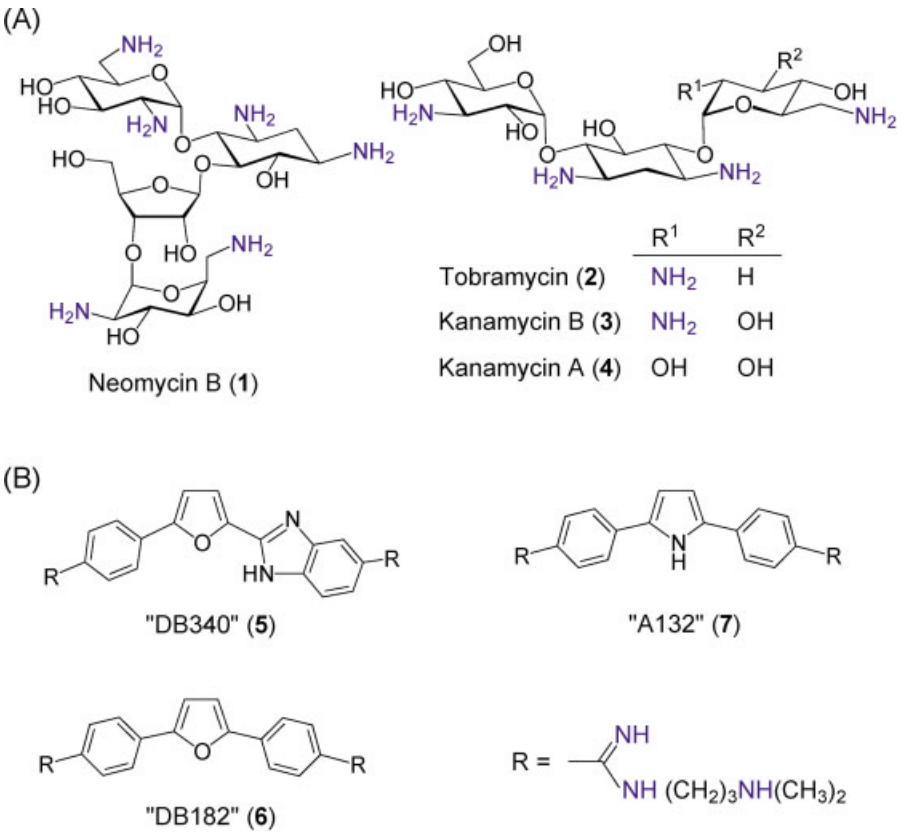


**FIGURE 8** Previously described inhibitors of Rev–RRE binding.[26,40] The aminoglycosides (A) differ, primarily, by the number and basicity of their amino groups (blue). The "aromatic diamidines" (B), on the other hand, are all tetracations, but differ by the identities of the unfused heterocyclic rings.[40]

($K_d$ = 0.24 $\mu M$), on a truncated RRE construct (RREIIB-TR Figure 5), is *not* disruptive to Rev binding ($K_i$ = 2.0 $\mu M$).[38] Indeed, we have recently used the same truncated RRE used by Marino (RREIIB-TR Figure 5), and have also found that for this particular RRE construct under our conditions, neomycin has a 10-fold higher affinity for its primary binding site ($K_d$ = 0.4 $\mu M$) as compared to the Rev binding site ($K_i$ = 3 $\mu M$).[37,38] The most likely explanation for this difference between RRE66 and RREIIB-TR is that the neomycin binding site is altered by the truncations made to the RRE66. Indeed, early footprinting experiments by Zapp indicate that neomycin binds near the three-way junction of Stem IIA, IIB, and IIC of the RRE66.[26] This region is dramatically altered by truncation of the RRE where stems IIA and IIC are removed (Figure 5). This minimization of the RRE appears to affect the mechanism by which neomycin displaces Rev from the RRE.

## SOLID-PHASE PEPTIDE DISPLACEMENT ASSAY

A novel biophysical method has been developed to characterize the affinity *and* specificity of Rev–RRE inhibitors.[39] The components of the assay are schematically shown in Figure 9 and include (a) insoluble agarose beads covalently modified with streptavidin, (b) a biotinylated RRE, and (c) the fluorescein-labeled Rev peptide RevFl. Assembly of these components forms an immobilized "ternary complex," where the biotinylated RRE binds to streptavidin, and RevFl binds to the RRE with the same dissociation constant that is measured in solution by fluorescence anisotropy ($K_d$ = 3 n$M$). Calculating the binding constant for RevFl and the RRE66 using the solid phase is slightly different than in solution, since the "surface volume" of the free RRE is the same as the surface volume of the Rev-RRE complex [Eq. (2)]:

$$K_d \text{ (on a surface)} = \frac{[\text{RRE}][\text{RevFl}]}{[\text{Complex}]} = \frac{(\text{Moles of free RRE})\,[\text{RevFl}]}{(\text{Moles of complex})} \quad (2)$$

The concentration of RevFl in the supernatant "[RevFl]" is calculated by comparing the fluorescence intensity of the supernatant to a calibration curve of RevFl concentration versus fluorescence emission in-

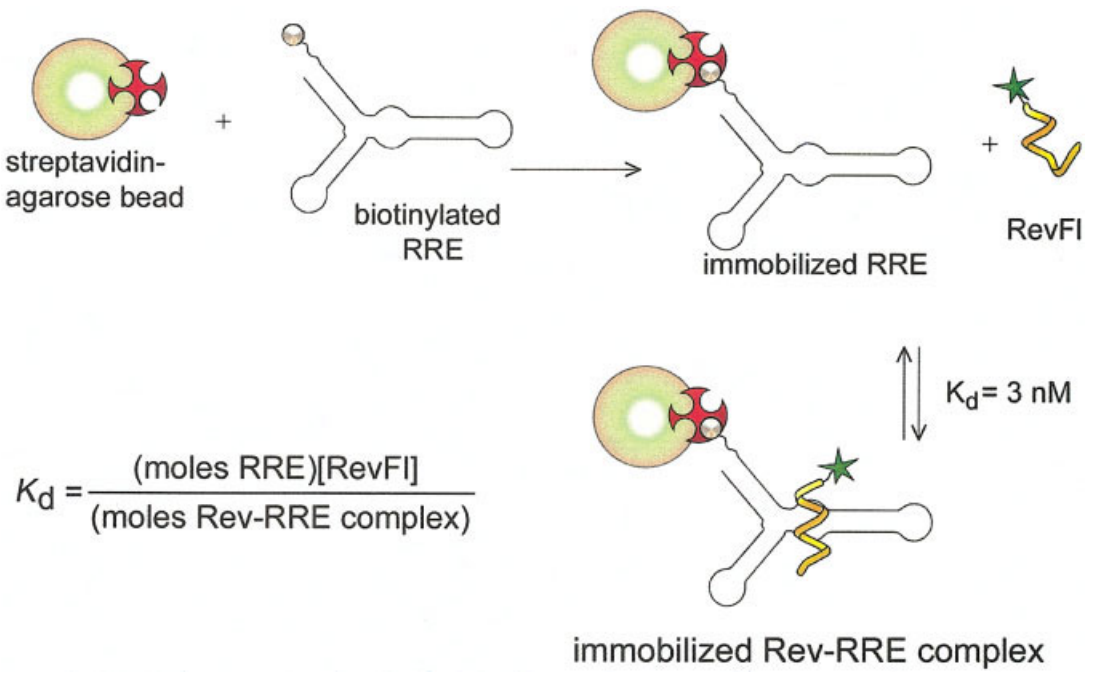


**FIGURE 9** Assembly of the immobilized Rev–RRE complex used for the solid-phase assay.[39]

tensity (Figure 6). The total moles of RNA on the solid support are determined during the immobilization of the biotinylated RRE: the uv absorbance of the supernatant is used to calculate the amount of RNA absorbed by the agarose/streptavidin gel (greater than 95% efficiency). The total moles of RRE bound by RevFl are determined by displacing RevFl from the solid support with 8*M* guanidinium hydrochloride, then quantifying the supernatant in a buffered solution. As in solution, RevFl binds to the immobilized RRE with high specificity. RevFl does not bind to the argarose/strapavidin gel that lacks the immobilized RRE. In addition, the immobilized Rev–RRE complex is not significantly disrupted by a large excess of $tRNA^{mix}$ or CT DNA (200-fold excess). Titration of the nonbiotinylated RRE or the unlabeled Rev peptide, however, efficiently displaces RevFl from the solid support ($IC_{50}$ = 90 n*M* and 35 n*M*, respectively).[39]

Following formation of the solid-phase immobilized RevFl–RRE complex, small molecule inhibitors are added, and the fraction of RevFl in solution is monitored as a function of inhibitor concentration (top of Figure 10). The concentration of inhibitor needed to displace half of the peptide (the $IC_{50}$ value) is measured in the presence and absence of an excess of competing nucleic acids (Figure 10). A comparison of these $IC_{50}$ values reflects the affinity of the small molecule to the Rev binding site on the RRE, vs its affinity to the binding sites presented by the competitor nucleic acids. To evaluate the RRE specificity of a small molecule, numerous mixtures of heterogeneous nucleic acids are used as competitors ($tRNA^{mix}$, CT DNA, etc.). Indeed, the RRE specificity, as we have defined it, is proportional to the Rev–RRE inhibitory activity of a ligand in the presence of "all" other potential targets [Eq. (1)]. To accelerate the selection of highly specific Rev–RRE inhibitors, the solid-phase assay could, in principle, be automated and/or conducted in the presence of cellular lysate. Most biophysical methods (including fluorescence anisotropy, surface plasmon resonance, NMR) are not amenable to the analysis of complex mixtures of biomolecules, making the examination of specificity an arduous task.

To examine the effectiveness and dependability of this solid-phase-based assay, two families of known Rev–RRE inhibitors have been evaluated: the aminoglycoside antibiotics and the aromatic diamidines (Figure 8).[26,40] Table I summarizes the $IC_{50}$ values obtained by the solid-phase assay in comparison to fluorescence anisotropy measurements. An excellent agreement between the two assays is observed for the aminoglycosides (Table I). We observe the same trend in relative activities of the aminoglycosides as reported by Zapp for displacement of the Rev protein from the RRE (neomycin B > tobramycin ≥ kanamycin B > kanamycin A).[26] Indeed, since aminoglycosides bind to RNA primarily through electrostatic interactions,[41,42] this same activity trend is reported for many other RNAs as well.[16,42,43]

For the aromatic diamidines, their previously reported trends in RRE affinity are also accurately reproduced by both assays (DB340 > DB182 > A132).[40] According to the solid-phase assay, how-

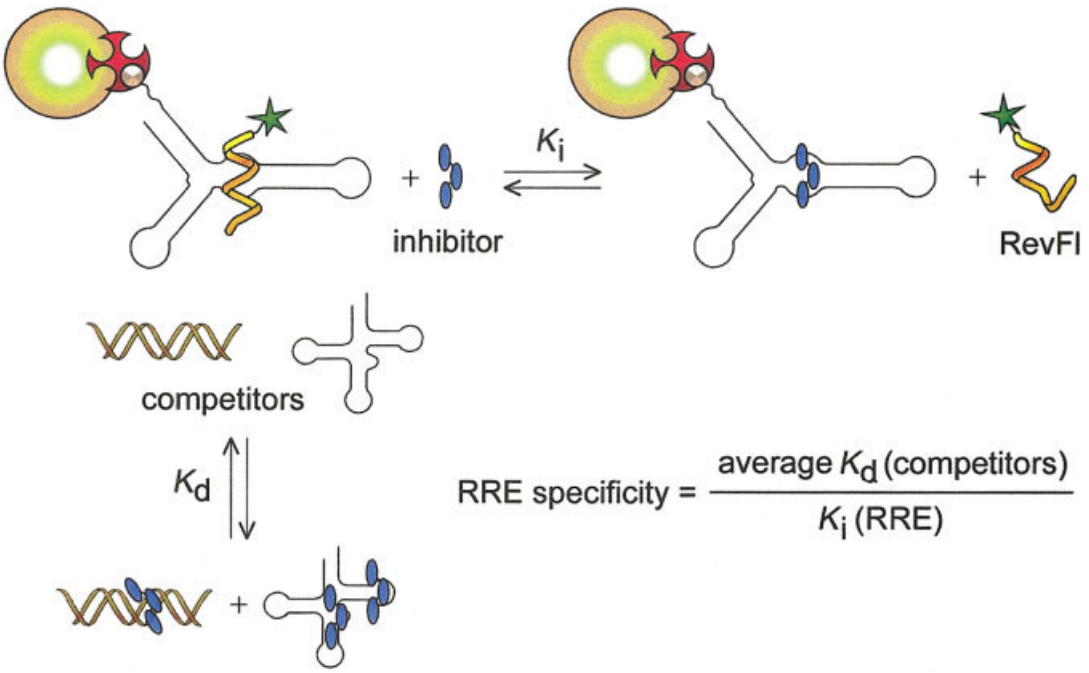


**FIGURE 10** Measuring the relative RRE specificity of a ligand in the presence of competing nucleic acids using the solid-phase assay.[39]

ever, the absolute $IC_{50}$ values for these compounds are 3–10-fold lower as compared to fluorescence anisotropy (Table I). Systematic discrepancies between $IC_{50}$ values determined by the solid-phase assay vs fluorescence anisotropy are, in this case, related to a general problem encountered when applying fluorescence anisotropy to binders that are either fluorescent or can quench fluorescence. Fluorescent inhibitors will themselves have a fluorescence anisotropy value. In addition, significant quenching of the RevFl peptide can affect the measured anisotropy (Figure 6). The solid-phase assay can easily adapt to these problems since the supernatant (containing the interfering inhibitor and displaced RevFl) can be removed, and the fluorescence remaining on the solid support can be quantified.[39] Native gel-shift mobility assays were conducted to confirm the $IC_{50}$ values of inhibitors that interfere with RevFl fluorescence. For these ligands, the $IC_{50}$ values obtained from the solid-phase assay are, indeed, more accurate than the $IC_{50}$ values derived from fluorescence anisotropy (Figure 11).

To evaluate the RRE specificity of the aminoglycosides and the aromatic diamidines, the $IC_{50}$ value of each compound is measured in the presence of different competing nucleic acids (Table I). Upon addition of DNA, no significant change in $IC_{50}$ values is seen for the aminoglycosides. This confirms the RNA over DNA selectivity of these compounds.[44,45] In the presence of a tRNA mixture, however, the aminoglycosides lose 2–3-fold of their activities, confirming their binding of tRNA (Table I).[46] Indeed, aminoglycosides are known to bind to and inhibit the function of a large number of unrelated RNAs with good through moderate activities ($IC_{50}$ = 0.1–100 $\mu M$).[16,42,43] Aminoglycosides typically have, therefore, a low specificity for RNA sites in this affinity range [Eq. (1)]. Aminoglycosides do, however, show excellent selectivity for RNA over DNA.[44,45] For this reason, we have used aminoglycosides as starting materials for the synthesis of new ligands that are targeted to specific RNA sites, including the RRE.[30,47]

In the absence of competing nucleic acids, all three of the aromatic diamidines are more potent Rev–RRE inhibitors than the aminoglycosides (Table I). In the presence of competing DNA, however, the $IC_{50}$ values of these compounds increase by 10-fold (Table I). This confirms the ability of these compounds to bind double-stranded DNA with high affinity.[48] Our data also indicate that these compounds have a moderate affinity to a mixture of tRNAs (Table I). Taken together, these results suggest that the aromatic diamidines are only moderately selective for the RRE. Wilson and colleagues have shown, however, that DB340 forms a well-defined, high-affinity complex with the RRE that has been partially characterized by NMR.[49] Interestingly, this compound binds as a dimer in the minor groove of a truncated version of RREIIB-TR.[49] Since Rev binds in the major groove of the RRE,[50] the displacement of Rev by DB340 likely involves an allosteric mechanism. Indeed, the RRE is a highly dynamic molecule that can adopt alternate conformations upon ligand binding.[51] The abil-

**Table I. $IC_{50}$ Values ($\mu$M) for Rev–RRE Inhibition and Anti-HIV Activities[a]**

| Compound | Anisotropy[b] | Solid Phase | Solid Phase with DNA[c] | Solid Phase with tRNA[d] | HIV-1 Inhibition[e] |
|---|---|---|---|---|---|
| Neomycin B (**1**) | 7 | 7 | 8 | 20 | > 30 |
| Tobramycin (**2**) | 47 | 45 | 50 | 100 | > 30 |
| Kanamycin B (**3**) | 80 | 90 | 90 | 170 | nd[f] |
| Kanamycin A (**4**) | 780 | 750 | 750 | 1200 | nd |
| DB340 (**5**) | 0.3 | 0.1 | 1.3 | 0.7 | nd |
| DB182 (**6**) | 1.5 | 0.4 | 4 | 0.8 | nd |
| A132 (**7**) | 10[g] | 1.2 | 10 | 3 | nd |
| Ethidium Bromide (**8**) | 0.6 | nd | nd | nd | 0.2 |
| Eilatin (**9**) | > 3 | nd | nd | nd | nd |
| $\Delta$-$[Ru(bpy)_2eilatin]^{2+}$ (**10**) | 0.9 | 2 | 50 | 2 | 0.8 |
| $\Delta$-$[Ru(bpy)_2eilatin]^{2+}$ (**11**) | 1.1 | 2 | 10 | 2 | 2.0 |
| $[Ru(bpy)_2pre\text{-}eilatin]^{2+}$ (**12**) | 20 | nd | nd | nd | 30 |
| $[Ru(bpy)_3]^{2+}$ (**13**) | 170[g] | > 10,000 | nd | nd | > 100 |

[a]Approximate deviation of all measurements is less than or equal to ± 35% of reported value.
[b]Using 10 n*M* RevFl and 100 n*M* RRE66.
[c]Includes 230 $\mu M$ (in bases) of plasmid DNA.
[d]Includes 230 $\mu M$ (in bases) of $tRNA^{mix}$ (Sigma type X).
[e]According to CD4+ HeLa plaque assay.
[f]Not determined.
[g]Significant fluorescence interference during course of titration.

ity of the RRE to rearrange upon the binding of small molecules may severely complicate the structure-based design of small molecules targeted towards this and other structurally characterized RNA sites.

## MEASURING SMALL MOLECULE–NUCLEIC ACID BINDING BY MONITORING THE PHOTOPHYSICAL CHANGES OF THE SMALL MOLECULE

A number of RRE ligands exhibit changes in their photophysical properties upon binding nucleic acids (Figure 12). In addition to fluorescence anisotropy (above), the uv-vis absorbance and/or fluorescence emission spectra of a ligand are routinely used to probe for RNA and DNA binding. For example, the fluorescence intensity of a 200 n*M* solution of ethidium bromide (**8**) increases as the RRE66 is titrated (Figure 13A). Using Scatchard analysis,[52] this data could, potentially, be fit to a single binding site with an affinity of $K_d$ = 110 n*M* (red squares, Figure 14). Unfortunately, the analysis of this type of binding data, even with nonlinear curve fitting, does not prove binding stoichiometry. For example, it is likely that ethidium's apparent RRE affinity ($K_d \approx$ 110 n*M*) represents two or more binding sites that have slightly different binding affinities, and may explain why the Scatchard plot is not perfectly linear (red squares, Figure 14). Ethidium is an effective inhibitor of Rev–RRE binding with an $IC_{50}$ of 600 n*M* (Table I); *if* a single ethidium binding site were responsible for the displacement of RevFl, this value would convert into a $K_i$ of 15 n*M*. Since this value is significantly lower

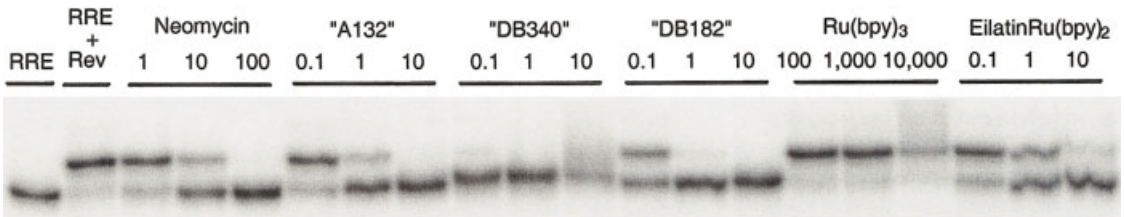


**FIGURE 11** Native gel-shift electrophoresis is used to visualize formation and subsequent inhibition of the Rev–RRE complex, thereby providing an orthogonal method to measure the approximate $IC_{50}$ values of Rev–RRE inhibitors. The numerical values indicate the concentration of each ligand ($\mu M$).[39]

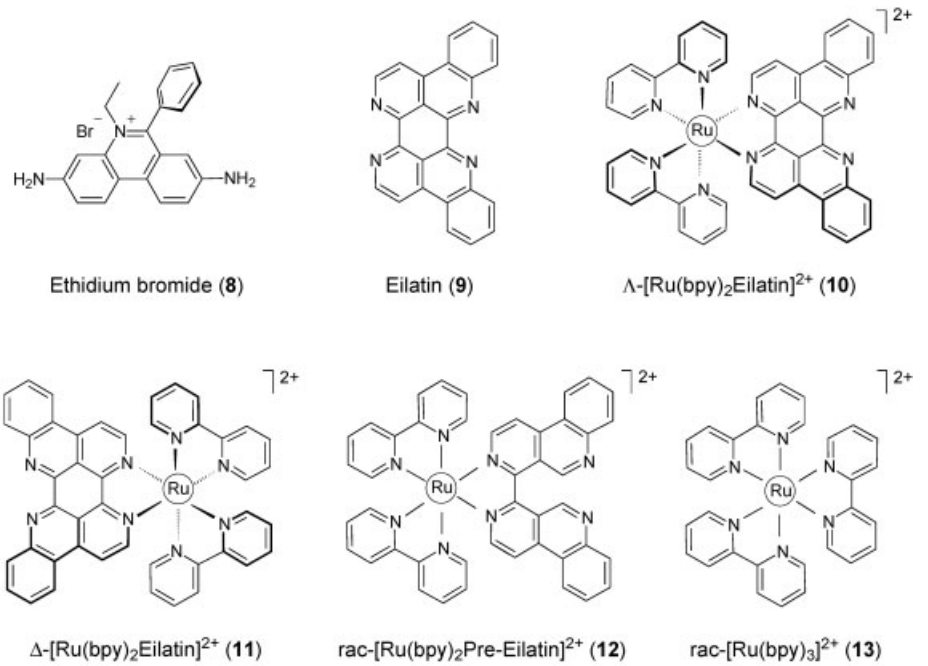


**FIGURE 12** Structures of newly described RRE ligands. Compounds **8–11** exhibit changes in their photophysical properties upon binding nucleic acids.

than the apparent binding affinity between ethidium and the RRE66, it is likely that more than one ethidium binding site on the RRE is capable of displacing RevFl. Indeed, RRE66 titrations conducted at higher concentrations of ethidium bromide (800 n*M*) suggest the presence of at least two binding sites with an average $K_d$ = 180 n*M* (blue triangles, Figure 14). A comparison of these Scatchard plots illustrates how the apparent stoichiometry of a binding interaction is critically dependent on the concentration of the observable species relative to the affinity of the RNA–ligand interaction being studied (Figure 14). In general, as the concentration of the fluorescent probe increases, its binding to lower affinity site(s) becomes more apparent in the isotherm. In the case of ethidium bromide binding the RRE, we interpret the binding data as indicative of two ethidium binding sites with slightly different affinities, ($K_{d1}$ = 80 n*M*, $K_{d2}$ = 280 n*M*). Indeed, RRE66 titrations conducted at 50 n*M* of ethidium bromide suggest the presence of a single binding site with a $K_d$ = 80 n*M* (not shown). In almost all cases, however, an orthogonal assessment of binding stoichiometry increases the confidence in the reported affinity.

Analysis of simple *two* component binding isotherms offers some advantages over the Rev displacement assays described above. From two component systems, binding affinities ($K_d$) are more easily extracted and provide more thermodynamically meaningful information than activity measures ($IC_{50}$ values). Monitoring the spectral properties of the small molecule, upon titration of the target RNA, does not, however, establish the functional inhibition of the RRE. Some small molecules, like eilatin (**9**), bind to the RRE with high affinity, but do not displace RevFl. The decrease in fluorescence intensity of a solution of eilatin upon titration of the RRE66 (Figure 13B) indicates the presence of one or more high-affinity binding sites with an apparent $K_d \approx 130$ n*M* (assuming a binding stoichiometry of 1:1). The titration of eilatin into a solution of RevFl and RRE indicates, however, that eilatin does not displace RevFl from the RRE (Figure 15B). This suggests that eilatin's high-affinity binding site(s) on the RRE are not disruptive to Rev binding. Ethidium bromide, on the other hand, shows better consistency between its affinity to RRE and its ability to displace Rev (Figure 15A). Eilatin appears to bind to the RRE in a different location than both RevFl and ethidium bromide, as it cannot displace either of these compounds from the RRE (through its solubility limit in water $\approx$ 3 $\mu M$).

## NEW RRE LIGANDS

We have used the solid-phase assay and fluorescent anisotropy to discover and characterize a number of new Rev–RRE inhibitors.[30,39,47] For example, when eilatin is incorporated into the enantiomeric octahedral metal complexes Δ- and Λ- $[Ru(bpy)_2eilatin]^{2+}$,

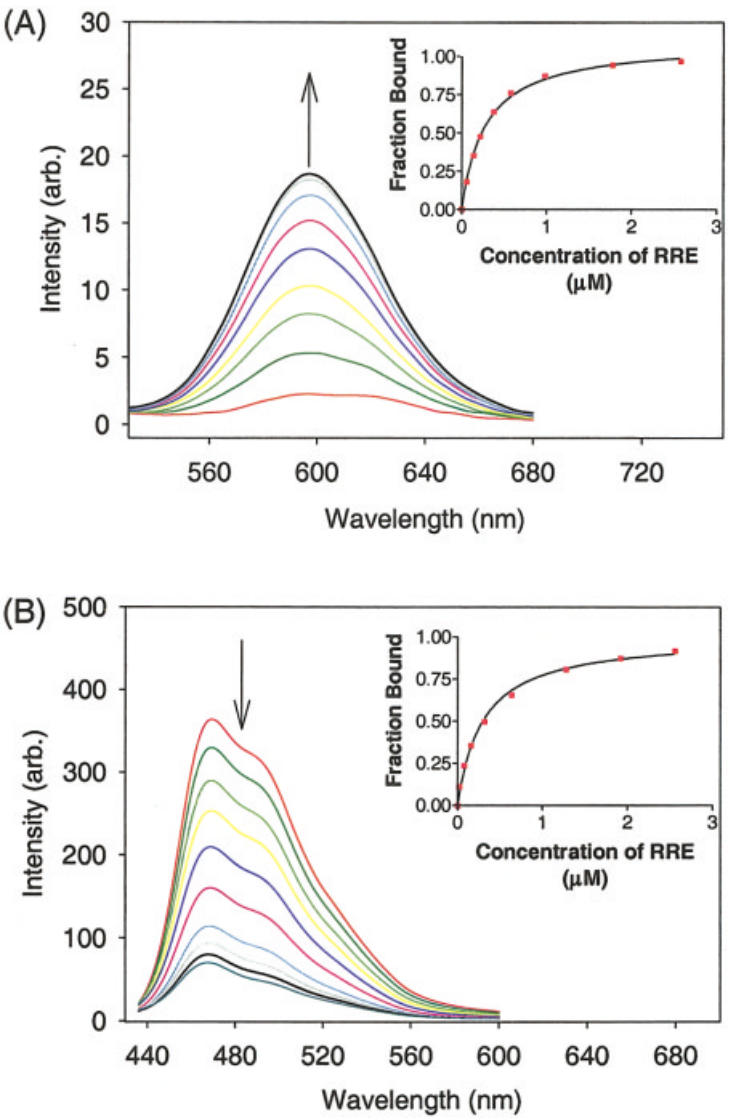


**FIGURE 13** Fluorescence emission spectra of a 200 n*M* solution of ethidium bromide (**8**) with increasing concentrations of RRE66 (excitation at 490 nm) (A). By taking the fractional change in emission intensity as equal to the fraction of ligand bound, the fraction of ethidium bound by the RRE can be computed (inset, A). Fluorescence emission spectra of a 200 n*M* solution of eilatin (**9**) with increasing concentrations of RRE66 (excitation at 400 nm) (B). By taking the fractional change in emission intensity as equal to the fraction of ligand bound, the fraction of eilatin bound by the RRE can be computed (inset, B). Additional details regarding experimental conditions are found in the caption to Figure 7.

it becomes an effective inhibitor of Rev–RRE binding (Figure 12 and Table I). These eilatin-containing metal complexes are more potent inhibitors than the most active natural aminoglycoside, neomycin B (Table I). Fluorescence anisotropy, the solid-phase assay, and native gel-shift electophoresis all indicate that each of the $[Ru(bpy)_2eilatin]^{2+}$ enantiomers are approximately 5-fold better Rev–RRE inhibitors than neomycin B (Figure 11 and Table I). Both the Δ- and Λ-enantiomers have approximately the same RRE affinities (Table I); but in the presence of DNA, the Λ-enantiomer loses its potency by a factor of 25, and the Δ-enantiomer by a factor of 5 (Table I). This indicates that the Λ-enantiomer has a higher affinity to double-stranded DNA as compared to the Δ-enantiomer. We have confirmed this finding through more direct experiments, including ethidium bromide displacement and thermal denaturation experiments with CT DNA.[53,54] Interestingly, in the presence of $tRNA^{mix}$, the potency of neither of the $[Ru(bpy)_2eilatin]^{2+}$ enantiomers is affected (Table I). This suggests that these compounds have a high RRE specificity relative

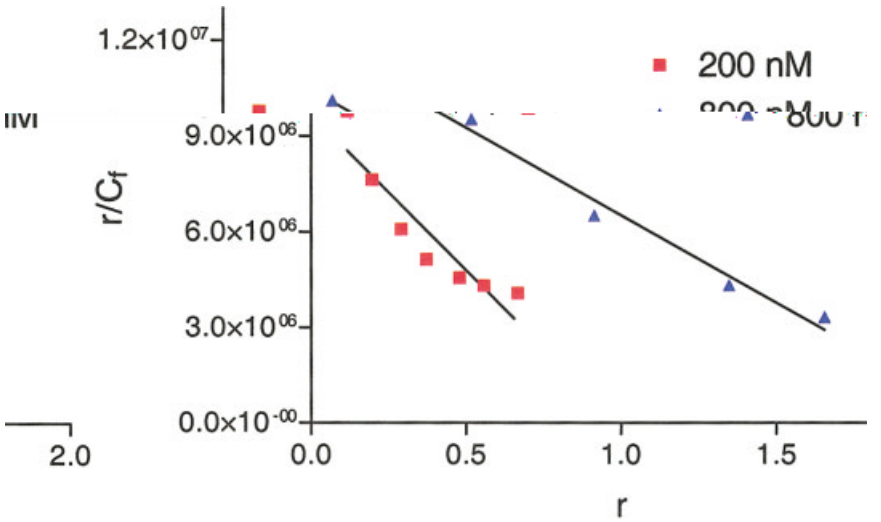


**FIGURE 14** Scatchard plots as determined by monitoring the fluorescence intensity of ethidium bromide bound upon addition of RRE66 (Figure 13A). Titrations were conducted at 200 n*M* of ethidium (red squares) or at 800 n*M* of ethidium bromide (blue triangles). The curved plot at 200 n*M* of ethidium may indicate the presence of two or more binding sites that have slightly different affinities. Nonlinear curve fitting was used to examine binding data collected at 50 n*M* of ethidium, which fit well to a single ethidium binding site with a $K_d$ = 80 n*M* (not shown).

to other RNA molecules, but *not* with respect to DNA. This is the exact opposite trend as observed for the aminoglycosides (Table I). Interestingly, we have recently monitored the uv-vis absorbance spectrum of the eilatin–Ru complexes as a function of nucleic acid concentration, and have discovered that these complexes have a significantly higher affinity to most *single-stranded* polymeric RNAs as compared *double-stranded* polymeric RNAs.[54] Once again, this is the exact opposite selectivity trend as reported for the aminoglycosides.[44]

The enantiomeric octahedral metal complexes Δ- and Λ-[Ru(bpy)$_2$eilatin]$^{2+}$ represent a new class of RRE ligands, where the RRE affinity and specificity can be tuned by the incorporation of different metal ligands. To examine the importance of the eilatin moiety (**9**) to the Rev–RRE inhibition activities of Δ- and Λ-[Ru(bpy)$_2$eilatin]$^{2+}$, we have investigated the activities of two related octahedral metal complexes **12** and **13** (Figure 12). These compounds have a much lower RRE affinity according to both Rev peptide and ethidium bromide displacement experiments.[53] Indeed, [Ru(bpy)$_3$]$^{2+}$ is over 10,000-fold less effective at Rev–RRE inhibition as compared to Δ- and Λ-[Ru(bpy)$_2$ eilatin]$^{2+}$ (Table I and Figure 11). Interestingly, there appears to be a correlation between the Rev–RRE inhibition activity of these four Ru(II) metal complexes and their respective anti-HIV activities (Figure 16 and Table I). We have also found, however, that compared to Δ- and Λ-[Ru(bpy)$_2$eilatin]$^{2+}$, compounds **12** and **13** display a much lower affinity to many other nucleic acids as well.[53] A general correlation exists, therefore, between the nucleic acid affinities of these compounds and their anti-HIV activities. This is, to the best of our knowledge, the first time that this type of correlation has ever been reported for HIV inhibition.

## HIV ASSAYS

We have employed orthogonal anti-HIV assays to monitor the fractional reduction in activity of the HIV-1 isolate X 794 LAI (group M) in human cell cultures. The HIV activity in CD4+ HeLa cells is quantified by a plaque-formation assay.[55] Plaques (or syncytia) are multinucleated cellular masses that are initiated by the expression of the ENV protein, which allows CD4+ cells to fuse with HIV-infected cells (Figure 2). Syncytia have been shown to be the primary cause of death in T-cell cultures.[56] The fractional decrease in the number of plaques as a function of **8**, **10**, **11**, **12**, and **13** was measured in CD4+ HeLa cells (Figure 16). There is a strong correlation between the anti-HIV activity and the Rev–RRE inhibition activity of compounds **8**, **10**, **11**, **12**, and **13** (Table I). This supports a possible relationship between the binding of nucleic acids and the anti-HIV activities of these compounds. This is not proof, however, that Rev–RRE inhibition is the primary mechanism responsible for the observed anti-HIV activities, as these assays will be sensitive to inhibition at many

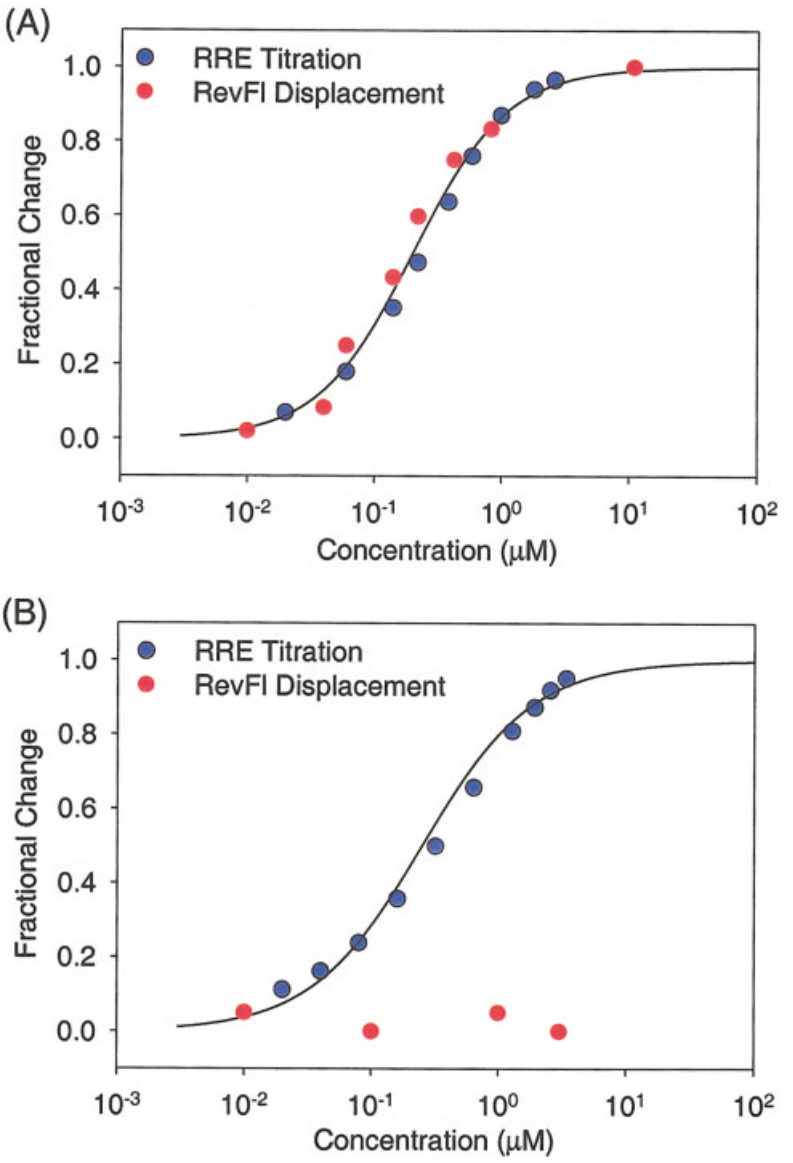


**FIGURE 15** (A) Binding of ethidium bromide (600 n*M*) to the RRE as determined by monitoring ethidium bromide's fluorescence intensity as a function of RRE concentration (blue circles) or by using ethidium bromide (**8**) to displace RevF1 from the Rev–RRE66 complex (red circles). (B) Binding of eilatin (200 n*M*) to the RRE as determined by monitoring the fluorescence intensity of eilatin (**9**) as a function of RRE66 concentration (blue circles) or by using eilatin to displace RevF1 from the Rev–RRE complex (10 n*M* each) (red circles).

different steps of the HIV life cycle (Figure 2). Unlike compounds **8** and **10–13**, we have *not* found a correlation between the Rev–RRE inhibition and anti-HIV activities of the aminoglycosides **1** and **2** (Table I). The likely reason for this is that aminoglycosides show very poor cellular uptake into the eukaryotic cells used for these assays.[35]

For compounds that *do* show promising activities in the HeLa plaque assay, a more traditional anti-HIV assay is conducted to confirm the ability of each compound to suppress HIV gene expression.[55] ELISA is used to quantify the fractional decrease in p24 expression in HIV-infected human peripheral blood monocytes.[55] We have employed this assay to evaluate the anti-HIV activities of five different compounds (including **2**, **8**, and **10**). Both the HeLa plaque assay and the p24 ELISA assay have yielded approximately the same $IC_{50}$ values for all compounds evaluated by both assays thus far. It should be noted, however, that the use of different cell types, different HIV strains, and higher multiplicity of infections, might yield different results that those presented in Figure 16.[59,60]

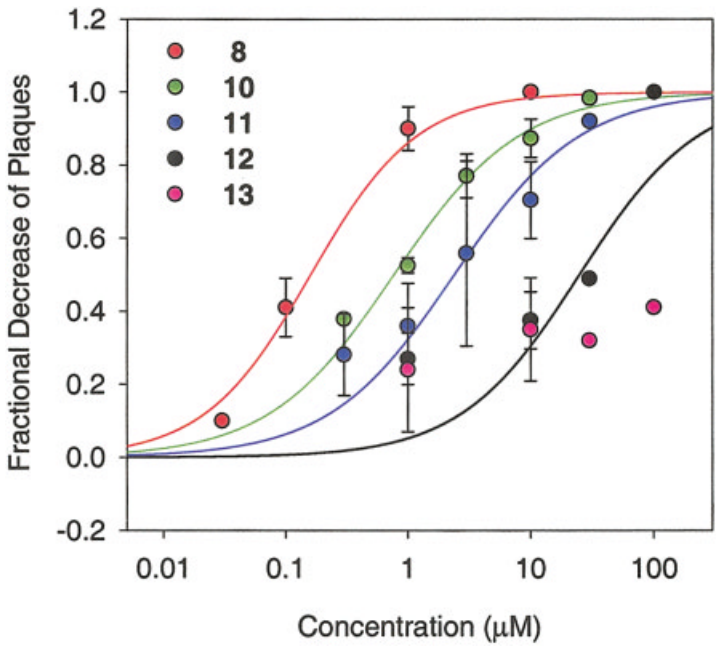


**FIGURE 16** The anti-HIV activities of compounds **8** and **10–13**, as evidenced by the fractional decrease in plaque (syncytia) formation in CD4+ HeLa cells. Compound **10** was also evaluated for anti-HIV activity in human peripheral blood monocytes (PBMC) by measuring the dose-dependent decrease in HIV-1 p24 expression using ELISA; this assay also yielded an $IC_{50} = 1\ \mu M$. For both assays, healthy cells are infected to a low multiplicity of infection (MOI $\approx$ 0.001). Inhibitory compounds are then added, and the cells are quantified for HIV activity following an additional three-day incubation. Unlike all the other compounds evaluated, compound **8** exhibits signs of toxicity at 10 $\mu$M (detachment of the HeLa cells from the culture plates). Error bars reflect the standard deviation of 2–4 replicates for each point. If a point lacks error bars, it is due to the small sampling conducted for these experiments as all points should have a minimum standard deviation of approximately $\pm$0.08 fractional change.

## CONCLUSIONS

Systematic studies of the binding interactions between small-molecule ligands and the RRE are essential for deciphering the parameters that govern effective RRE recognition and inhibition. Fluorescence-based assays are important new tools to examine these interactions. Problems can arise, however, when evaluating inhibitors that are themselves fluorescent or quenchers of fluorescence. These problems can be overcome by using orthogonal methods for evaluating new ligands, including the spectroscopic observation of the small molecule upon titration of the target RNA. This type of two-component binding study can elucidate the RNA affinity and stoichiometry of the ligand, but it does not establish the functional inhibition of the RRE. In vitro Rev displacement experiments continue, therefore, to serve as an important tool for evaluating the functional inhibition of the RRE. These methods should continue to find utility in identifying and characterizing new drug-like molecules that possess anti-HIV activities.

We thank Ken Blount and Lev Elson-Schwab for their critical evaluations of the manuscript, and Haim Weizman for his assistance with artwork. We would also like to thank W. D. Wilson and D. W. Boykin for sharing the aromatic diamidines, and M. Kol and D. Gut for eilatin and the eilatin-containing metal complexes. Financial support was provided by the Universitywide AIDS Research Program (ID01-SD-027) and the National Institutes of Health (AI 47673).

## REFERENCES

1. Gestland, R. F.; Cech, T. R.; Atkin, J. F., Eds.; The RNA World; Cold Spring Harbor Laboratory Press: Cold Spring Harbor, NY, 1999.
2. Kornberg, A.; Baker, T., Eds.; DNA Replication; W. H. Freeman: New York, 1992.
3. Green, R.; Noller, H. F. Annu Rev Biochem 1997, 66, 679–716.
4. Blackburn, E. H. In RNA Structure and Function; Cold Spring Harbor Laboratory Press: Cold Spring Harbor, NY, 1998; pp 669–693.

5. Nilsen, T. W. In RNA Structure and Function, Cold Spring Harbor Laboratory Press: Cold Spring Harbor, NY, 1998; pp 279–307.
6. Hentze, M. W.; Kuhn, L. C. Proc Natl Acad Sci USA 1996, 93, 8175–8182.
7. Lau, N. C.; Lim, L. P.; Weinstein, E. G.; Bartel, D. P. Science 2001, 294, 858–862.
8. Werstuck, G.; Green, M. R. Science 1998, 282, 296–298.
9. Winkler, W.; Nahvi, A.; Breaker, R. R. Nature 2002, 419, 952–956.
10. Nahvi, A.; Sudarsan, N.; Ebert, M. S.; Zou, X.; Brown, K. L.; Breaker, R. R. Chem Biol 2002, 9, 1043–1049.
11. Fields, B. N.; Knipe, D. M.; Howley, P. M., Eds. Fundamental Virology; Lippincott–Raven: Philadelphia, PA, 1996.
12. De Clereq, E. Biochem Biophys Acta 2002, 1587, 258–275.
13. Wilson, W. D.; Li, K. Curr Med Chem 2000, 7, 73–98.
14. Sucheck, S. J.; Wong, C.-H. Curr Opin Chem Biol 2000, 4, 678–686.
15. Cheng, A. C.; Calabro, V.; Frankel, A. D. Curr Opin Struct Biol 2001, 11, 478–484.
16. Michael, K.; Tor, Y. Chem Eur J 1998, 4, 2091–2098.
17. Frankel, A. D.; Young, J. A. T. Annu Rev Biochem 1998, 67, 1–25.
18. Gait, M. J.; Karn, J. Trends Biochem Sci 1993, 18, 255–259.
19. Pollard, V. W.; Malim, M. H. Annu Rev Microbiol 1998, 52, 491–532.
20. Li, C. J.; Friedman, D. J.; Wang, C.; Metelev, V.; Pardee, A. B. Science 1995, 268, 429–431.
21. Mann, D. A.; Mikaelian, I.; Zemmel, R. W.; Green, S. M.; Lowe, A. D.; Kimura, T.; Singh, M.; Butler, P. J.; Gait, M. J.; Karn, J. J Mol Biol 1994, 241, 193–207.
22. Iwai, S.; Pritchard, C.; Mann, D. A.; Karn, J.; Gait, M. J. Nucleic Acids Res 1992, 20, 6465–6472.
23. Malim, M. H.; Tiley, L. S.; McCarn, D. F.; Rusche, J. R.; Hauber, J.; Cullen, B. R. Cell 1990, 60, 675–683.
24. Schaal, H.; Klein, M.; Gehrmann, P.; Adams, O.; Scheid, A. J Virol 1995, 69, 3308–3314.
25. Chen, J.-H.; Le, S.-Y.; Maizel, J. V. Nucleic Acids Res 2000, 28, 991–999.
26. Zapp, M. L.; Stern, S.; Green, M. R. Cell 1993, 74, 969–978.
27. Wang, Y.; Hamasaki, K.; Rando, R. R. Biochemistry 1997, 36, 768–779.
28. Bentley, K. L.; Thompson, L. K.; Klebe, R. J.; Horowitz, P. M. BioTechniques 1985, 3, 356–365.
29. Pope, A. J.; Haupts, U. M.; Moore, K. J. Drug Discovery Today 1999, 4, 350–362.
30. Kirk S. R.; Luedtke, N. W.; Tor Y. J Am Chem Soc 2000, 122, 980–981.
31. Daly, T. J.; Cook, K. S.; Gray, G. S.; Maione, T. E.; Rusche, J. R. Nature 1989, 342, 816–819.
32. Heaphy, S.; Dingwall, C.; Ernberg, I.; Gait, M. J.; Green, S. M.; Karn, J.; Lowe, A. D.; Singh, M.; Skinner, M. A. Cell 1990, 60, 685–693.
33. Cho, J.; Rando, R. R. Biochemistry 1999, 39, 8548–8554.
34. Tok, J. B.; Dunn, L. J.; Des Jean, R. C. Bioorg Med Chem Lett 2001, 11, 1127–1131.
35. Luedtke, N. W. Ph.D. thesis, University of California, San Diego, 2003.
36. Wang, Y.; Hamasaki, K.; Rando, R. R. Biochemistry 1997, 36, 768–779.
37. Luedtke, N. W.; Tor, Y., in preparation.
38. Lacourciere, K. A.; Strivers, J. T.; Marino, J. P. Biochemistry 2000, 39, 5630–5641.
39. Luedtke, N. W.; Tor, Y. Angew Chem Intl Ed 2000, 39, 1788–1790.
40. Xiao, G.; Kumar, A.; Li, K.; Rigl, C. T.; Bajic, M.; Davis, T. M.; Boykin, D. W.; Wilson, W. D. Bioorg Med Chem 2001, 1097–1113.
41. Orval, B. C.; Stage, T. K.; Uhlenbeck, O. C. Biochemistry 1995, 34, 11186–11190.
42. Wong, C.-H.; Hendrix, M.; Priestly, E. S.; Greenberg, W. A. Chem Biol 1998, 5, 397–406.
43. Walter, F.; Vicens, Q.; Westhof, E. Curr Opin Chem Biol 1999, 3, 694–704.
44. Chen, Q.; Shafer, R. H.; Kuntz, I. D. Biochemistry 1997, 36, 11402–11407.
45. Mei, H.-Y.; Galan, A. A.; Halim, N. S.; Mack, D. P.; Moreland, D. W.; Sanders, K. B.; Truong, H. N.; Czarnik, A. W. Bioorg Med Chem Lett 1995, 5, 2755–2760.
46. Kirk, S. R.; Tor, Y. Bioorg Med Chem 1999, 7, 1979–1991.
47. Luedtke, N. W.; Baker, T. J.; Goodman, M.; Tor, Y. J Am Chem Soc 2000, 122, 12035–12036.
48. Wang, L.; Bailly, C.; Kumar, A.; Ding, D.; Bajic, M.; Boykin, D. W.; Wilson, W. D. Proc Natl Acad Sci USA 2000, 97, 12–16.
49. Li, K.; Davis, T. M.; Bailly, C.; Kumar, A.; Boykin, D. W.; Wilson, W. D. Biochemistry 2001, 40, 1150–1158.
50. Battiste, J. L.; Mao, H.; Rao, N. S.; Tan, R.; Muhandiram, D. R.; Kay, L. E.; Frankel, A. D.; Williamson, J. R. Science 1996, 273, 1547–1551.
51. Hung, L. W.; Holbrook, E. L.; Holbrook, S. R. Proc Natl Acad Sci USA 2000, 97, 5107–5112.
52. Scatchard, G. Ann NY Acad Sci 1949, 51, 660–672.
53. Luedtke, N. W.; Hwang, J. S.; Glazer, E. C.; Gut, D.; Kol, M.; Tor, Y. Chembiochem 2002, 3, 766–771.
54. Luedtke, N. W.; Hwang, J. S.; Nava, E.; Gut, D.; Kol, M.; Tor, Y., submitted.
55. Richman, D. D.; Johnson, V. A.; Mayers, D. L.; Shirasaka, T.; O'Brien, M. C.; Mitsuya, H. In Current Protocols in Immunology; John Wiley & Sons: New York 1993; Suppl 8, Unit 12.9, pp 1–21.
56. Sylwester, A.; Murphy, S.; Shutt, D.; Soll, D. R. J Immunol 1997, 158, 3996–4007.
57. Tan, R.; Chen, L.; Buettner, J. A.; Hudson, D.; Frankel, A. D. Cell 1993, 73, 1031–1040.
58. Auer, M.; Gremlich, H.-U.; Seifert, J.-M.; Daly, T. J.; Parslow, T. G.; Casari, G.; Gstach, H. Biochemistry 1994, 33, 2988–2996.
59. Erika, N. Yonago Igaku Zasshi 1988, 39, 438–447.
60. Hui, Y.; Ptak, R.; Paulman, R.; Pallansch, M.; Tom Chang, C-W. Tetrahedron Lett 2002, 43, 9255–9257.